S-Parameter Characterization of Submicrometer Low-Voltage Organic Thin-Film Transistors

Tarek Zaki, *Student Member, IEEE*, Reinhold Rödel, Florian Letzkus, Harald Richter, Ute Zschieschang, Hagen Klauk, *Member, IEEE*, and Joachim N. Burghartz, *Fellow, IEEE*

***Abstract*— This letter presents the first comprehensive experimental studies on the frequency response of staggered low-voltage organic thin-film transistors (OTFTs) using S-parameter measurements. The transistors utilize air-stable dinaphtho-thieno-thiophene as the organic semiconductor with various channel lengths and gate overlaps. A peak cutoff frequency of 3.7 MHz for a channel length of 0.6 μm, gate overlap of 5 μm, and a supply voltage of 3 V is achieved. In view of the low supply voltage and air-stability, this result marks a record achievement in OTFT technology. The channel length dependence of the cutoff frequency is described in a compact model and a close correspondence to the measured data of OTFTs with variable device dimensions is shown. Moreover, the cutoff frequencies at different gate biases are found to be proportional to the dc transconductance.**

***Index Terms*— Cutoff frequency, organic thin-film transistors, scattering parameters, semiconductor device modeling.**

I. Introduction

ORGANIC thin-film transistors (OTFTs) are providing impetus in large-area, light-weight, and mechanically flexible applications, such as backplanes, for flexible displays and radio-frequency identification tags [1], [2]. Analysis of the frequency response of OTFTs is of great interest to gain deeper insight into the physics of the device and for comparing device structures as well as assessing materials-related limitations. So far, the frequency limit has been derived from the propagation delay of a ring oscillator, which only provides an average delay figure [3]. Given the variability of state-of-the-art OTFTs, this characterization method is not fully satisfactory. Therefore, cutoff frequency measurements on stand-alone OTFTs have been explored, using direct measurement of the gate and drain modulation currents [4]. Such user-configured measurement setup, involving multiple test instruments, is cumbersome and makes the extraction of device parasitics very difficult. Therefore, a self-contained method for characterizing the cutoff frequency of OTFTs by means of S-parameter measurements is highly desirable, as demonstrated on other thin-film transistor types, such as ZnO TFTs [5]. In this letter, to the best of our knowledge, we present the first report on S-parameter measurements of OTFTs.

Manuscript received December 22, 2012; revised February 4, 2013; accepted February 6, 2013. Date of publication March 7, 2013; date of current version March 20, 2013. This work was supported in part by the German Research Foundation under Grant BU 1962/4-1. The review of this letter was arranged by Editor A. Chatterjee.

T. Zaki and J. N. Burghartz are with the University of Stuttgart, Stuttgart 70569, Germany, and also with the Institute for Microelectronics Stuttgart, Stuttgart 70569, Germany (e-mail: zaki@ines.uni-stuttgart.de).

R. Rödel, U. Zschieschang, and H. Klauk are with the Max Planck Institute for Solid State Research, Stuttgart 70569, Germany.

F. Letzkus and H. Richter are with the Institute for Microelectronics Stuttgart, Stuttgart 70569, Germany.

Color versions of one or more of the figures in this letter are available online at http://ieeexplore.ieee.org.

Digital Object Identifier 10.1109/LED.2013.2246759

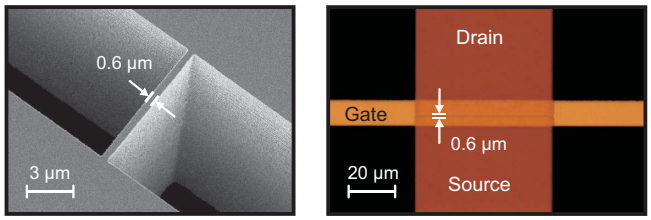

(a) (b)

Fig. 1. (a) SEM image of a silicon stencil mask used to pattern the source and drain contacts of an OTFT. (b) Top-view photograph of a top-contact OTFT with a channel length of 0.6-μm fabricated on a glass substrate.

OTFTs in practical applications require simultaneously low-voltage operation, high bandwidth, small parasitics, and good air-stability. Recent record results are cutoff frequencies of 28 MHz for fullerene C_{60} (*n*-type; not air-stable) TFTs and 11 MHz for pentacene (*p*-type) TFTs having channel lengths of 2 μm and operating, however, at a large supply voltage of 25 V [4]. Others have reported cutoff frequencies of 2 MHz for poly(3-hexylthiophene) (*p*-type) TFTs with a channel length of 480 nm at 10 V and 1.6 MHz for pBTTT (*p*-type) TFTs with a channel length of 200 nm at 8 V [6], [7]. Here, we report a record cutoff frequency with respect to a low supply voltage of only 3 V for dinaphtho[2, 3-b:2', 3'-f]thieno[3, 2-b]thiopheneDNTT (*p*-type) TFTs. An important advantage of DNTT over pentacene and poly(3-hexylthiophene) is its good air stability [8], [9]. Using silicon stencil masks, we have fabricated inverted staggered (bottom-gate, top-contact) DNTT TFTs with submicrometer features down to 0.6 μm and very small contact resistance without exposing the semiconductor layer to potentially harmful solvents during device processing [10]. Gate dielectrics based on ultrathin self-assembled monolayers (SAMs) have been utilized to enable the low-voltage operation ($\leq$3 V) [10]. A close correspondence between the dc and ac characteristics has been achieved, and an adopted model to describe the dependence of the cutoff frequency on the channel length is presented.

II. OTFT Fabrication

Referring to Fig. 1, the transistors were fabricated on an alkali-free glass substrate. Aluminum gates (30-nm thick), the semiconductor DNTT (20-nm thick), and gold source/drain contacts (25-nm thick) were all deposited in vacuum and patterned using silicon stencil masks. Prior to the semiconductor deposition, the substrate with the aluminum gates was briefly exposed to an oxygen plasma to create a 3.6-nm-thick AlO_x layer and then immersed into a 2-propanol solution

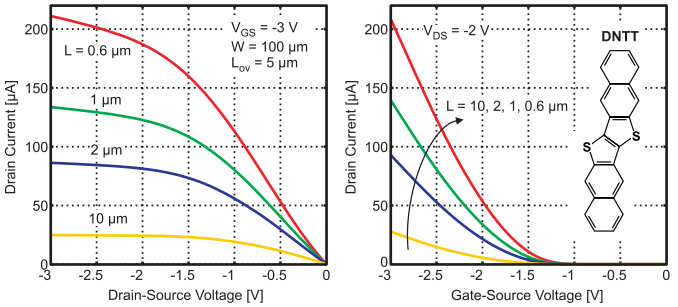

Fig. 2. (a) Measured static output characteristics. (b) Measured static saturation transfer characteristics. The inset shows the molecular structure of the organic semiconductor DNTT. The figures depict that by reducing the channel length of the TFTs, the drain current is increased. From the transfer characteristic, effective saturation mobilities of 1.9, 1.2, 0.8, and 0.7 cm^2/Vs are extracted for channel lengths of 10, 2, 1, and 0.6 μm, respectively.

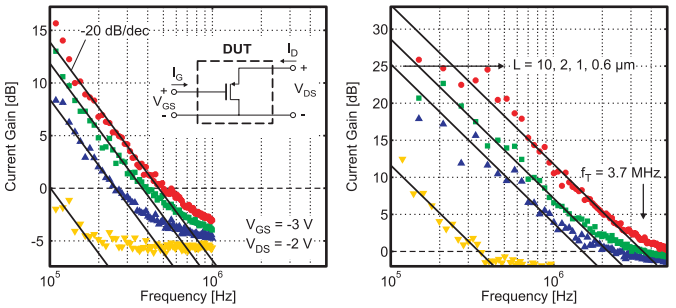

Fig. 3. Current gains versus frequency derived from calibrated full two-port S-parameter measurements on OTFTs with a channel width of 100 μm and channel lengths of 10, 2, 1, and 0.6 μm. (a) Gate overlap of 20 μm. (b) Gate overlap of 5 μm. The inset shows the OTFT as a device under test (DUT) for the vector network analyzer (VNA), where Port 1 is connected to the gate and Port 2 is connected to the drain, while the source is common ground.

of tetradecylphosphonic acid to form a 1.7-nm-thick SAM, resulting in a 5.3-nm-thick hybrid (AlO_x/SAM) gate dielectric with a unit area capacitance (C_I) of about 900 nFcm^{-2}. The channel width (W) of all the TFTs is 100 μm, the channel length (L) is 10, 2, 1, or 0.6 μm, and the gate overlap (L_{ov}) is 20 or 5 μm. The intrinsic mobility (μ_o) of the semiconductor was found to be 2.5 cm^2/ Vs.

III. Electrical Characterization

Measured static drain currents of the OTFTs with the various channel lengths and a gate overlap of 5 μm are shown in Fig. 2. The on/off current ratios of the OTFTs range from 10^7 to 10^5 for channel lengths of 10 to 0.6 μm, respectively. Measurements reveal that the extracted effective saturation mobility (μ_{eff}) is decreased as the channel length is reduced. This is owed to the increase in the relative contribution of the contact resistances to the total device resistance [11]. The relationship between these parameters will be explained further below. Furthermore, the OTFTs feature promising shelf-life, bias-stress stability, matching, and hysteresis behavior as demonstrated thoroughly in [9] and [10].

Full two-port scattering S-parameter measurements that relate the ac currents and voltages between the drain and the gate contacts were carried out using an HP 3577A vector network analyzer (VNA) at frequencies up to 5 MHz. All measurements were performed on-chip, in ambient air and at room temperature. The de-embedding procedure using a 12-term error correction model was employed to remove the impact of the parasitics associated with the measurement setup and on-chip contacts [12]. Accordingly, the standard short, open, through and matched loads are utilized to remove those parasitics to obtain the S-parameters at the device terminals.

The de-embedded S-parameters constitute a complete set of coefficients sufficient to describe the electrical behavior between the inputs and outputs of the OTFTs. Correspondingly, the short circuit small-signal current gains ($h_{21} = i_D/i_G$) are derived from the measured S-parameters at a gate-source voltage (V_{GS}) of –3 V and drain-source voltage (V_{DS}) of –2 V for OTFTs with channel lengths of 10, 2, 1, and 0.6 μm and gate overlaps of 20 and 5 μm (Fig. 3). As depicted in the figure, the current gain h_{21} decays with a slope of –20 dB/decade, resulting from the total gate impedance given by $1/j\omega C_G$, where C_G is the total gate capacitance. This validates the measurement procedure and verifies that the transistors follow the conventional FET-like behavior. At high frequencies, the decay levels off due to the zero in the transfer function h_{21}, which denotes a current flow through the relatively large gate-drain capacitance (C_{GD}).

In this configuration, the dynamic performance of the transistors is quantified by the current-gain cutoff frequency (f_T), defined as the frequency at which the current gain is unity ($|h_{21}| = 1$) and given in the saturation regime by

$$f_T = \frac{g_m}{2\pi C_G} = \frac{\mu_{\text{eff}}(V_{GS} - V_{TH})}{2\pi L(2L_{ov} + (2/3)L)} \tag{1}$$

where g_m, V_{GS}, and V_{TH} are the transconductance, gate-source voltage, and threshold voltage, respectively. Note that for transistors with short channels and large gate overlaps, C_G in (1) has to account for additional fringe currents flowing at the periphery of the intrinsic transistor. In principle, the cutoff frequency is improved by having large carrier mobility, small channel length, and small gate overlap. Therefore, the cutoff frequencies extracted from all OTFTs tested are plotted in Fig. 4(a) to investigate the impact of channel length and gate overlap on f_T. As expected, the cutoff frequency is found to increase with reduced channel lengths and/or gate overlaps, and a maximum $f_T = 3.7$ MHz was obtained for an OTFT with $L = 0.6$ μm and $L_{ov} = 5$ μm. The solid and dotted lines represent f_T calculated from (1) using two different representations for μ_{eff}. It is shown that for a constant μ_{eff} (dotted lines), the results are overestimated for shorter channels. This is attributed to the contact resistance (R_C), the influence of which becomes more dominant at smaller channel lengths. Thus, assuming an ohmic contact resistance, the effective mobility in saturation can be written as

$$\mu_{\text{eff}} = \frac{2\mu_o L}{2L + \mu_o W C_I R_C (V_{GS} - V_{TH}).} \tag{2}$$

This formula above is adopted from [13] and derived in the same way except that the device is assumed to be symmetric, while the impact of R_C on both V_{GS} and V_{DS} is considered. A reliable and good matching of the model to the experimental data has been obtained for a threshold voltage of $\sim$ –1.2 V and a contact resistance of $\sim$0.1 kΩcm. The value of R_C is smaller than was previously reported in [11], which was extracted by the transmission line method (TLM) in the linear operation regime. This is owed to the reduction of the transfer length (L_T) at larger absolute drain-source

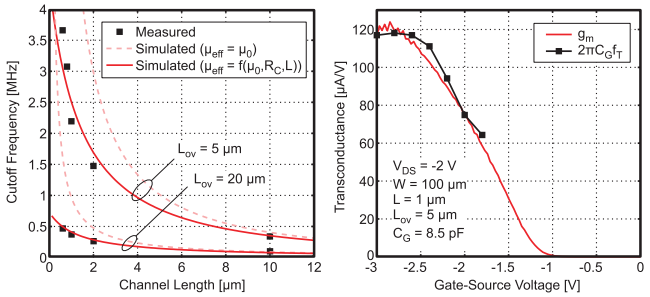

Fig. 4. (a) Summary of the unity current-gain cutoff frequencies f_T extracted for different channel lengths (L) and gate overlaps (L_{ov}). The dotted line represents simulated f_T with a constant effective mobility (μ_{eff}) that is equal to the intrinsic mobility. The solid line represents the simulated f_T with an effective mobility that is channel-length dependent, providing excellent agreement with the measured data. (b) Measured f_T and dc transconductance (g_m) as a function of gate-source voltage. A total gate capacitance (C_G) of 8.5 pF is extracted from the linear dependence between f_T and g_m. The figure confirms the close correspondence between the dc and ac measurements.

voltages, i.e., L_T is considerably smaller in the saturation regime than in the linear regime as demonstrated by the measurements and simulations in [11] and [14], respectively. Given that $R_C \cdot W = 2R_{\text{sheet}} L_T \coth(L_{ov}/L_T)$, where R_{sheet} is the sheet resistance of the semiconductor layer, the transfer length is defined as the characteristic length over which 63% of the charge-carrier exchange between the contacts and the semiconductor occurs ($R_{\text{sheet}} = 250\,\text{k}\Omega\,\text{sq}^{-1}$, $L_T \leq 4\ \mu$m) [11].

The correspondence between the dc and ac characteristics has been examined. Given that $\mu_{\text{eff}} = 0.8$ cm^2/Vs and $V_{TH} = -1.1$ V from the static transfer characteristics of the OTFT with $L = 1\ \mu$m and $L_{ov} = 5\ \mu$m, R_C can be similarly reproduced from (2) to be $\sim$0.1 kΩcm. The extracted value is identical to the aforementioned result determined from the S-parameter measurements. Furthermore, Fig. 4(b) shows the cutoff frequencies extracted from the S-parameter measurements (multiplied by a constant $2\pi C_G$) at different gate biases along with the dc transconductance (extracted from static saturation transfer characteristics) for the OTFT with $L = 1\ \mu$m and $L_{ov} = 5\ \mu$m. The linear dependence between both quantities matches with (1), and a gate capacitance (C_G) of 8.5 pF can be extracted. From the device geometry, $C_G \simeq$ 9.6 pF is calculated, which is in excellent agreement with the extracted value.

Finally, the validity of this characterization approach by measuring S-parameters has been verified, to be published later, on OTFTs based on another p-type organic semiconductor, namely, 2, 9-didecyldinaphtho[2,3-b:2', 3'-f]thieno[3,2-b]thiophene (C_{10}-DNTT).

IV. Conclusion

We, for the first time, demonstrated S-parameter-based characterization of organic TFTs. Moreover, in view of the low 3-V supply voltage, a record cutoff frequency of 3.7 MHz was measured on a DNTT air-stable OTFT with a channel length and a gate overlap of 0.6 and 5 μm, respectively. The submicrometer patterning and reduced parasitics were attributed to the thin-film evaporation through high-resolution silicon stencil masks. The deviation of the measured cutoff frequencies for short channels owing to device contacts was physically modeled and a good fit to the measured data of OTFTs with various channel lengths and gate overlaps was accomplished. By varying the gate-source voltage, the linear dependence between the measured cutoff frequencies and the dc transconductance was verified. Our results showed that the OTFT technology can well be extended to the submicrometer range and that high-frequency characterization of OTFTs by means of S-parameter measurements is feasible, which helps in extracting the parasitics present in the device and in building accordingly an OTFT small-signal equivalent circuit.

Acknowledgment

The authors gratefully acknowledge J. Digel of the Institute of Electrical and Optical Communications Engineering (Prof. M. Berroth), University of Stuttgart, for assistance in high-frequency characterization.

References

[1] N. Yoneya, H. Ono, Y. Ishii, K. Himori, N. Hirai, H. Abe, A. Yumoto, N. Kobayashi, and K. Nomoto, "Flexible electrophoretic display driven by solution-processed organic thin-film transistors," *J. Soc. Inf. Display*, vol. 20, no. 3, pp. 143–147, Mar. 2012.

[2] K. Myny, S. Steudel, S. Smout, P. Vicca, F. Furthner, B. van der Putten, A. K. Tripathi, G.H. Gelinck, J. Genoe, W. Dehaene, and P. Heremans, "Organic RFID transponder chip with data rate compatible with electronic product coding," *Org. Electron.*, vol. 11, no. 7, pp. 1176–1179, Jul. 2010.

[3] K. Fukuda, T. Sekitani, T. Yokota, K. Kuribara, T. Huang, T. Sakurai, U. Zschieschang, H. Klauk, M. Ikeda, H. Kuwabara, T. Yamamoto, K. Takimiya, K.-T. Cheng, T. Someya, "Organic pseudo-CMOS circuits for low-voltage large-gain high-speed operation," *IEEE Electron Dev. Lett.*, vol. 32, no. 10, pp. 1448–1450, Oct. 2011.

[4] M. Kitamura and Y. Arakawa, "High current-gain cutoff frequencies above 10 MHz in n-channel C_{60} and p-channel pentacene thin-film transistors," *Jpn. J. Appl. Phys.*, vol. 50, no. 1, pp. 01BC01-1–01BC01-4, Jan. 2011.

[5] B. Bayraktaroglu, K. Leedy, and R. Neidhard, "Microwave ZnO thin-film transistors," *IEEE Electron Dev. Lett.*, vol. 29, no. 9, pp. 1024–1026, Sep. 2008.

[6] V. Wagner, P. Woebkenberg, A. Hoppe, and J. Seekamp, "Megahertz operation of organic field-effect transistors based on poly(3-hexylthiopene)," *Appl. Phys. Lett.*, vol. 89, no. 24, pp. 243515-1–243515-3, Dec. 2006.

[7] M. Caironi, Y.-Y. Noh, and H. Sirringhaus, "Frequency operation of low-voltage, solution-processed organic field-effect transistors," *Semicond. Sci. Tech.*, vol. 26, no. 3, pp. 034006-1–034006-8, Mar. 2011.

[8] U. Zschieschang, F. Ante, T. Yamamoto, K. Takimiya, H. Kuwabara, M. Ikeda, T. Sekitani, T. Someya, K. Kern, and H. Klauk, "Flexible low-voltage organic transistors and circuits based on a high-mobility organic semiconductor with good air stability," *Adv. Mater.*, vol. 22, no. 9, pp. 982–985, Mar. 2010.

[9] U. Zschieschang, F. Ante, D. Kälblein, T. Yamamoto, K. Takimiya, H. Kuwabara, M. Ikeda, T. Sekitani, T. Someya, J. Blochwitz-Nimoth, and H. Klauk, "Dinaphtho[2,3-b:2',3'-f]thieno[3,2-b]thiophene (DNTT) thin-film transistors with improved performance and stability," *Org. Electron.*, vol. 12, no. 8, pp. 1370–1375, May 2011.

[10] F. Ante, F. Letzkus, J. Butschke, U. Zschieschang, K. Kern, J. N. Burghartz, and H. Klauk, "Submicron low-voltage organic transistors and circuits enabled by high-resolution silicon stencil masks," in *Proc. IEEE Int. Electron Dev. Meeting*, Dec. 2010, pp. 21.6.1–21.6.4.

[11] F. Ante, D. Kälblein, T. Zaki, U. Zschieschang, K. Takimiya, M. Ikeda, T. Sekitani, T. Someya, J. N. Burghartz, K. Kern, and H. Klauk, "Contact resistance and Megahertz operation of aggressively scaled organic transistors," *Small*, vol. 8, no. 1, pp. 73–79, Jan. 2012.

[12] J. Fitzpatrick, "Error models for systems measurement," *Microw. J.*, vol. 21, no. 5, pp. 63–66, May 1978.

[13] A. Benor and D. Knipp, "Contact effects in organic thin film transistors with printed electrodes," *Org. Electron.*, vol. 9, no. 2, pp. 209–219, Apr. 2008.

[14] C.-W. Sohn, T.-U. Rim, G.-B. Choi, and Y.-H. Jeong, "Analysis of contact effects in inverted-staggered organic thin-film transistors based on anisotropic conduction," *IEEE Trans. Electron Dev.*, vol. 57, no. 5, pp. 986–994, May 2010.